International Journal of Computational Fluid Dynamics, Vol. 19, No. 1, January 2005, 79–86

Taylor & Francis
Taylor & Francis Group

On the limiters of two-equation turbulence models

CHANG HWAN PARK and SEUNG O PARK*

Department of Aerospace Engineering, Korea Advanced Institute of Science and Technology, 373-1 Kusong-Dong, Yusong-Gu, Daejeon 305-701, South Korea

(Received 3 July 2003; revised 27 May 2004)

When two-equation turbulence models are used, unrealistically large values of turbulence variables can appear due to the infringement of a realizability condition or to numerical error. To cure this in practical calculations, various limiters on the source terms are often employed. In the present work, a mathematically correct bound for eddy viscosity is obtained from the realizability condition itself. From this, realizability bounds for several terms of model equations are given. The effects of various bounds including the present one, are investigated on the predictions of fundamental flows including simple shear flows, supersonic compression ramp flow and supersonic base flow. It is shown that the limiter affects the prediction very significantly.

Keywords: Realizability condition; Realizability bounds; Limiters; Two-equation turbulence model; Numerical robustness

1. Introduction

When use is made of various two-equation turbulence models, we often adopt limiters on some terms for robust computation or for more realistic predictions. Durbin (1996) proposed a realizability bound of the turbulent time scale T to prevent anomalous growth of turbulent kinetic energy (TKE) in stagnation region. It was applied to standard eddy-viscosity based turbulence models and $\overline{v^2} - f$ model with considerable success (Behnia *et al.* 1998, Medic and Durbin 2002). Menter (1993) imposed the limit on the production term of TKE equation, which eliminated the unrealistic buildup of eddy viscosity in stagnation regions and removed the occurrence of spikes in the eddy viscosity due to numerical wiggles. Zheng and Liu (1995) and Liu and Zheng (1996) adopted a lower limit of the specific dissipation rate of the $k - \omega$ equation to improve numerical robustness. In fact, the use of limiters is widely adopted primarily to prevent blow up of solutions in practical computations.

In spite of the fact that various forms of limiters are employed in predictions with two-equation models, the effects of limiters on the solution have not been examined systematically. In this work, we first focus on the eddy viscosity to suggest a new bound and secondly investigate the effects of various limiters on the prediction of flows. For the latter, we present computational results for the case of simple shear flows, a supersonic compression ramp flow and a supersonic base flow.

2. Various limiters

In linear two-equation turbulence models, the eddy viscosity and the Reynolds stress are modeled by

$$\nu_t = C_\mu u^2 T \tag{1}$$

$$\overline{u_i' u_j'} = -2\nu_t S_{ij} + \frac{2}{3} k \delta_{ij}, \quad \text{with} \quad S_{ij} = \frac{1}{2}\left(\frac{\partial u_i}{\partial x_j} + \frac{\partial u_j}{\partial x_i}\right) \tag{2}$$

where u^2 is the velocity scale and T is the turbulence time scale. In the $k - \varepsilon$ model, $u^2 = k$ and $T = k/\varepsilon$. From equation (2), we see that when the strain rate is greater than a certain value, the normal component of the Reynolds stress can become negative. Negative normal stress can lead to an over-prediction of TKE resulting from very small value of dissipation rate, and finally over-prediction of eddy viscosity. This phenomenon is known to arise in the stagnation point flows (Durbin 1996, Behnia *et al.* 1998, Moore and Moore 1999, Medic and Durbin 2002) and in shock-wave/boundary-layer-interaction

*Corresponding author. Email: sopark@kaist.ac.kr; sopark@sop1.kaist.ac.kr

International Journal of Computational Fluid Dynamics
ISSN 1061-8562 print/ISSN 1029-0257 online © 2005 Taylor & Francis Ltd
http://www.tandf.co.uk/journals
DOI: 10.1080/10618560412331286292

(SWBLI) flows (Thivet *et al.* 2001, Thivet 2002). Excessive eddy viscosity results in very large values of skin friction and heat transfer coefficients. In Thivet (2002)'s simulation of 3-D SWBLI flow, the grid convergence could not be obtained because of unrealistically large value of eddy viscosity.

A most significant numerical problem is the appearance of nonphysical negative values of turbulence variables and various approaches have been devised to deal with this problem. The implementation of limiters (Ilinca and Pelletier 1998) and the use of discretization schemes that helps to preserve positivity such as linearization and implicit treatment of source terms (Jacon and Knight 1994, Shur *et al.* 1995) are typical approaches. However, even if the positivity of turbulent variables is guaranteed, it does not necessarily guarantee the boundness of turbulent variables. Consequently, computation can still lead to unphysically low levels of dissipation rate resulting in excessively large value of eddy viscosity (Liu and Zheng 1996, Luo *et al.* 1997) as is often the case in turbulent/non-turbulent interfaces. The specific dissipation rate $\omega(=\varepsilon/k)$ is so small in this region that the small error of strain rate tensor can yield erroneous spike in eddy viscosity (Menter 1993).

Ilinca and Pelletier (1998) suggested the following "clipping operator" to ensure the positivity of turbulence variables.

$$\begin{aligned}&\text{If } k \text{ is too small, it is replaced by } k_{\max}/d_k.\\ &\text{If } \varepsilon \text{ is too small, it is replaced by } \rho C_\mu (k^2/d_\mu \mu_l).\end{aligned} \tag{3}$$

Here, $k_{\max}$ is the maximum of k within the calculation domain, μ_l the laminar viscosity, and d_k and d_μ are the constants determined by a user.

Menter (1993) suggested a limiter on the production term of k in his shear stress transport (SST) model, which is

$$P_k = \min(P_k, C_l D_k), \quad \text{with} \quad C_l = 20 \tag{4}$$

where D_k is the dissipation term of TKE equation. In numerical simulations of transonic RAE airfoil and ejector nozzle, Kral *et al.* (1996) tested this limiter for low-Reynolds number $k-\varepsilon$ models, and acquired improved results. They also tested the limiter using values of 10, 20 and 50 for C_l, and found that the choice of C_l did not affect the overall solutions.

Zheng and Liu (1995) derived the following lower bound for the specific dissipation rate ω from the Schwartz inequality to improve computational robustness.

$$\omega \geq \frac{\sqrt{3}}{2}\sqrt{2\left(S_{ij}-\frac{1}{3}\frac{\partial u_k}{\partial x_k}\delta_{ij}\right)\frac{\partial u_i}{\partial x_j}} \tag{5}$$

Durbin (1996) and Durbin and Petersen Reif (2001) suggested the following bound on the eddy viscosity from the realizability condition to avoid an excessive k in the stagnation point flow.

$$\nu_t \leq \alpha \frac{1}{\sqrt{6}}\frac{k}{|S|}, \quad \text{with} \quad \alpha = 1, \quad |S| \equiv \sqrt{S_{ij}S_{ji}} \tag{6}$$

He also presented the bounds for turbulent time and length scales. Behnia *et al.* (1996, 1998) used $\alpha = 0.5$ or 0.6 to obtain a better result in the simulation of impinging jet flow with $\overline{\nu^2}-f$ model. Thivet *et al.* (2001) used $\alpha = 0.5$ in the simulation of SWBLI flow. Medic and Durbin (2002) used $\alpha = 0.6$ in the simulation of turbine blade flow.

Menter (1993)'s SST correction is

$$\begin{aligned}&\nu_t \leq \frac{a_1 k}{\sqrt{2}|W|}, \quad \text{with} \quad a_1 = 0.31,\\ &|W| = \sqrt{-W_{ij}W_{ji}}, \quad W_{ij} = \frac{1}{2}\left(\frac{\partial u_i}{\partial x_j}-\frac{\partial u_j}{\partial x_i}\right)\end{aligned} \tag{7}$$

It is known that the SST correction largely improved the prediction of two-equation model in adverse pressure gradient boundary layer. However, the SST correction is not an appropriate limiter for the flow with irrotational strain field such as a stagnation point flow, since the eddy viscosity bound becomes very large as $|W|$ approaches zero. Recently, Moore and Moore (1999) suggested a limiter that include both strain rate and rotation rate.

3. Eddy viscosity bound

Reynolds stress and eddy viscosity are given by equations (1) and (2). The TKE production rate is

$$P_k = 2\nu_t S_{ij} S_{ji} \tag{8}$$

Following Durbin (1996), as the rate of strain tensor S_{ij} becomes purely diagonal in principal axes coordinates, we have

$$\lambda_1^2 + \lambda_2^2 + \lambda_3^2 = |S|^2 \tag{9}$$

where λ_α's are the eigenvalues of S_{ij}.

For incompressible flow, the continuity equation requires that

$$\lambda_1 + \lambda_2 + \lambda_3 = S_{ii} = 0 \tag{10}$$

From equations (9) and (10), the following inequality holds.

$$|\lambda_\alpha| \leq \sqrt{\frac{2}{3}}|S| \tag{11}$$

If we write the Reynolds stresses in the principal axis coordinate, we have

$$\overline{u_\alpha^2} = -2\nu_t\lambda_\alpha + \frac{2}{3}k \tag{12}$$

Imposing the realizability constraint, $0 \leq \overline{u_\alpha^2} \leq 2k$, onto equation (12) yields

$$2\nu_t \max_\alpha \lambda_\alpha \leq \frac{2}{3}k \tag{13}$$

Here, $\max \lambda_\alpha$ refers to the maximum value of λ's.

Durbin (1996) chose $\max \lambda_\alpha$ to be the limit value given by equation (11) to obtain

$$\nu_t \leq \frac{1}{\sqrt{6}}\frac{k}{|S|} \tag{14}$$

Consequently, the following bounds follow.

$$T \leq \frac{1}{\sqrt{6}}\frac{1}{C_\mu u^2}\frac{k}{|S|} \tag{15}$$

$$P_k \leq \sqrt{\frac{2}{3}}k|S| \tag{16}$$

While equation (11) is correct, choice of $\max \lambda_\alpha$ from equation (11) to determine the eddy viscosity bound (equation (13)) is not logical in the following sense. If there exists a lowest bound of $\max \lambda_\alpha$, it is proper to use that bound to determine the eddy viscosity bound. To search for this lowest bound of $\max \lambda_\alpha$, we proceed as follows.

Equations (9) and (10) represent respectively the sphere of radius $|S|$ and a plane passing through the origin of the coordinate. The intersection of the sphere and the plane is the circle of radius $|S|$ centered at the origin as shown in figure 1. The coordinate of a point on this circle is $(\lambda_1, \lambda_2, \lambda_3)$. To examine the bound values of λ, we consider a general 3-D space. Let $(\lambda_1, \lambda_2, \lambda_3)$ be the coordinate of an arbitrary point. We easily see that the points that satisfy $\max \lambda_\alpha = a$ ($\alpha = 1, 2, 3$) are the points on the tetrahedron like surface of figure 2. The coordinate of the apex is (a,a,a) and each surface extends to infinity in the negative direction. We now note that the equilateral triangle ABC of figure 2 lies on the plane $\lambda_1 + \lambda_2 + \lambda_3 = 0$. Therefore, if the triangle ABC is inscribed in the circle of figure 1, the minimum bound of a is obtained, and if the circle circumscribes with the external triangle,

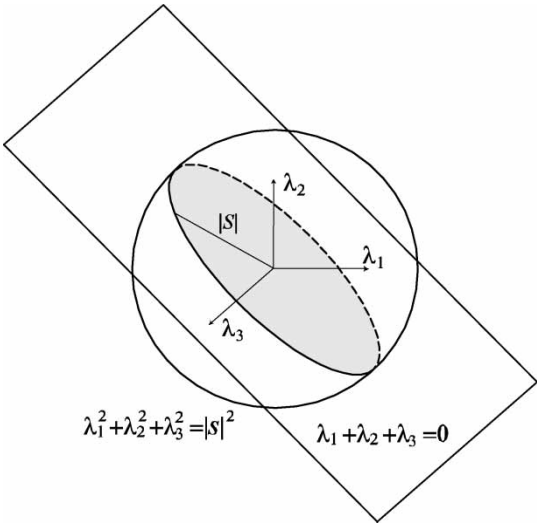

Figure 1. Schematic of the plane of intersection.

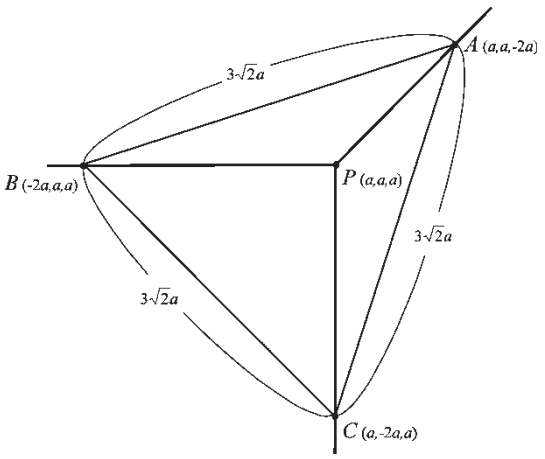

Figure 2. Three-dimensional geometry illustrating $\max \lambda_\alpha = a$ (λ_α is arbitrary).

the maximum bound is defined, as shown in figure 3. From the geometric relations depicted in figure 3, we readily find that

$$\sqrt{\frac{1}{6}}|S| \leq \max \lambda_\alpha \leq \sqrt{\frac{2}{3}}|S| \tag{17}$$

By adopting the minimum bound from equation (17), we have the following eddy viscosity bound.

$$\nu_t \leq \sqrt{\frac{2}{3}}\frac{k}{|S|} \tag{18}$$

Subsequently, the following bounds follow

$$T \leq \sqrt{\frac{2}{3}}\frac{1}{C_\mu u^2}\frac{k}{|S|} \tag{19}$$

$$P_k \leq \sqrt{\frac{8}{3}}k|S| \tag{20}$$

Note that these new bounds are twice as large as those proposed by Durbin.

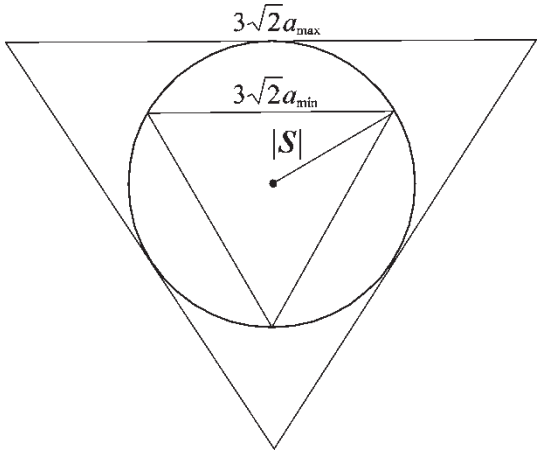

Figure 3. Intersection of the strain rate circle of figure 1 and the continuity plane of figure 2.

The eddy viscosity bound of equation (18) could also have been obtained from the Schwartz inequality as Zheng and Liu (1995) did to obtain the lower limit of ω. The Schwartz inequality $\left(\overline{u'_\alpha u'_\beta}\right)^2 \le \overline{u'^2_\alpha}\cdot\overline{u'^2_\beta}$ $(\alpha, \beta = 1, 2, 3)$ can be extended to

$$\overline{u'_i u'_j}\cdot\overline{u'_j u'_i} \le (2k)^2 \tag{21}$$

by summing for α, β. If equation (21) is invoked to the constitutive relation of equation (2), we again obtain the eddy viscosity bound of equation (18), which supports that our inference using geometrical relations is correct.

For compressible flow, we often adopt the following relation.

$$u''_i u''_j = -2\nu_t \hat{S}_{ij} + \frac{2}{3}k\delta_{ij} \tag{22}$$

$$\hat{S}_{ij} = S_{ij} - \frac{1}{3}\frac{\partial U_k}{\partial x_k}\delta_{ij} \tag{23}$$

The variable with a tilde denotes a Favre-averaged quantity. Since $\hat{S}_{ij}$ is traceless, the same relations of equations (9) and (10) hold for $\hat{S}_{ij}$. Thus, various bounds can be readily obtained.

The production term for the compressible flow case can be written as

$$P_k = P_{ki} - P_{kc} = 2\nu_t \hat{S}_{ij}\hat{S}_{ji} - \frac{2}{3}k(\nabla\cdot\vec{V}) \tag{24}$$

Note that P_{ki} takes the same formula as equation (8). Hence bounds for P_{ki} and P_{ki}/ε can be written as follows.

$$\frac{P_{ki}}{\varepsilon} = 2C_\mu \tilde{S}^2 \le \frac{4}{3}\frac{1}{C_\mu} \tag{25}$$

$$\tilde{S} \equiv \frac{k|S|}{\varepsilon} \le \sqrt{\frac{2}{3}}\frac{1}{C_\mu} \tag{26}$$

4. Effect of limiters

The bound of equation (18) is the least condition that any linear two-equation model should be subjected to. Thus, equation (18) or equations (19) and (20) can be used in two-equation models without any penalty since these are most general bounds. To investigate the effects of various limiters including the present one, computations were carried out for some simple flows. For convenience, we designate the limit given by equations (18) and (20) by R-0 limiter. The limit given by equation (6) with $\alpha = 0.6$ is designated as R-1 limiter, and with $\alpha = 0.5$ as R-2 limiter. For the Navier–Stokes computations of supersonic compression ramp flow and supersonic base flow, the clipping operator of equation (3) was employed with $d_k = 10^{15}$ and $d_\mu = 10^{-3}$, and the results are presented with the designation "no limiter".

4.1 Flat plate boundary layer and mixing layer

Form equations (25) and (26), bounds of non-equilibrium factor P_{ki}/ε and non-dimensional strain rate $\tilde{S}$ can be estimated. Strictly speaking, these equations give a bound for C_μ. However, by fixing C_μ, we may get estimates of P_{ki}/ε and $\tilde{S}$ for practical purpose. With $C_\mu = 0.09$, $P_{ki}/\varepsilon \le 14.8$ and $\tilde{S} \le 9.07$. It is known that $P_{ki}/\varepsilon \approx 1$ for flat plate boundary layer and $P_{ki}/\varepsilon \approx 1.8$ in homogeneous shear flow (Durbin and Petersen Reif 2001), and according to Menter (1993), P_{ki}/ε is not greater than 2 for most of shear flows. Therefore we find that the adoption of R-0 limiter would not affect the solution in most shear flows. However, solutions can be affected by R-1 and R-2 limiters, since these make P_{ki}/ε bounded by 1.33 and 0.93, respectively.

To provide an example, an incompressible flat plate boundary layer was calculated by using Wilcox (1998)'s EDDYBL code. The Launder–Sharma (LS) turbulence model (Launder and Sharma, 1974) was employed. Figure 4 depicts the eddy viscosity distribution predicted by the LS model. From the computed flow field, the bounded values of ν_t for R-0, R-1, and R-2 limiters can be calculated, which are sketched in figure 4. We see that the eddy viscosity bounds from R-0 and R-1 limiters are greater than the eddy viscosity of the LS model. Hence, the solution would not be affected by either R-0 or R-1 limiters. However, R-2 limiter generates the bound smaller than the computed eddy viscosity. Therefore, if R-2 limiter were employed, we would have smaller eddy viscosity to result in a reduced skin friction coefficient.

For an incompressible plane mixing layer, Wilcox (1998)'s MIXER code with the high Reynolds number standard $k-\varepsilon$ model predicts a spreading rate of 0.098. The experimental value is 0.115. Use of R-1 limiter yielded the spreading rate of 0.093, which implies that the eddy viscosity was affected by the limiter. When R-0 limiter was imposed, no change in the solution was observed as expected.

4.2 Compression ramp flow

The simulation of supersonic 3-D single and double sharp fin flow (Thivet *et al.*, 2001, Thivet 2002) indicated that there are irrealizable regions resulting from the large strain rate. Having this in mind, we selected the supersonic compression ramp flow with 20° wedge angle as a test case. The freestream Mach number was 2.79. A 2-D Navier–Stokes solver (Lee and Park 2002) with the LS turbulence model was used for the prediction of this flow. The computational domain, non-dimensionalized with the inlet boundary layer thickness δ_i, extended from -2 (upstream) to 6 (downstream) from the ramp corner along the wall and from 0 to 4 along the wall-normal direction. A 100×60 grid was used after the grid-test, and the grid point closest to the wall was kept below $y^+ = 1$. Inlet conditions for the mean flow variables and the turbulence variables were obtained from a 2-D compressible boundary layer code.

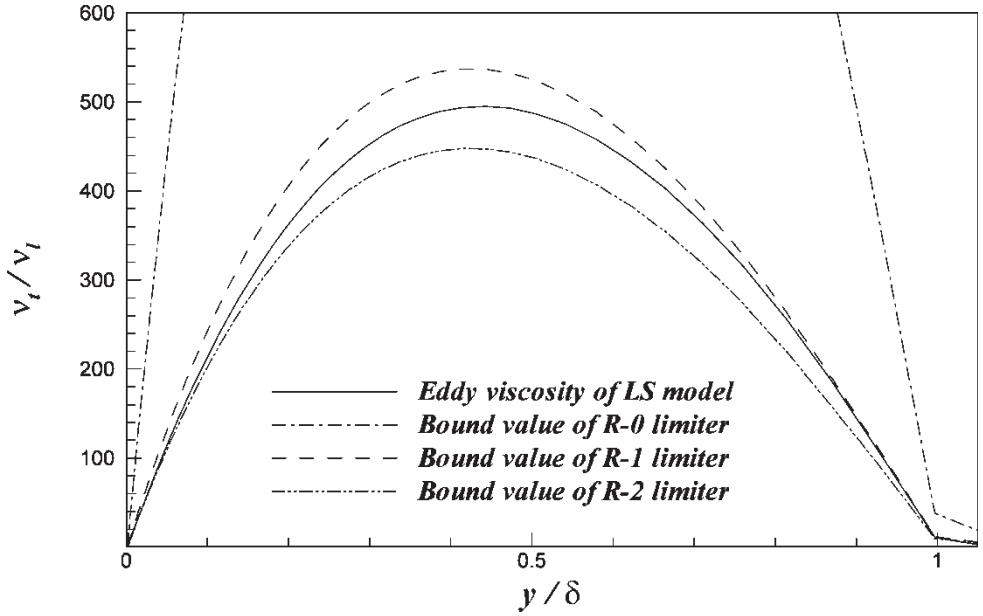

Figure 4. Eddy viscosity and limit value distributions of flat plate boundary layer.

The inlet velocity profile (from the boundary layer code) was generated to yield the momentum thickness Reynolds number of 93800 to match with the experimental data.

The skin friction coefficients are shown in figure 5 together with the experimental data (Smits and Muck 1987). It is known that two-equation turbulence models fail to predict adequately the supersonic compression ramp flows, and especially, they predict the skin friction and heat transfer higher than those measured in the downstream of reattachment (Yoon *et al.*, 1997, Wilcox 1998, Thivet *et al.*, 2001, Thivet 2002) as can be seen in figure 5. Figure 5 shows further that the predictions vary widely depending on the limiters chosen, especially in the downstream region of reattachment. As for Menter's production limiter, we see that the skin friction coefficient varies depending on the C_l value. The limit posed by equation (25), an equivalent to R-0 limiter, corresponds to the case of $C_l = 14.8$ if $C_\mu = 0.09$.

We note that the R-1 limiter yields the skin friction coefficient closer to the experimental value in the downstream of reattachment due to a severer restriction on the eddy viscosity than the R-0 limiter. However, it affects greatly the separation region such that the size of the separation region becomes larger than the experimental value. It was reported that the SST correction of Menter and the R-1 limiter predicted nearly the same result for the case of 2-D transonic bump flow (Thivet 2002).

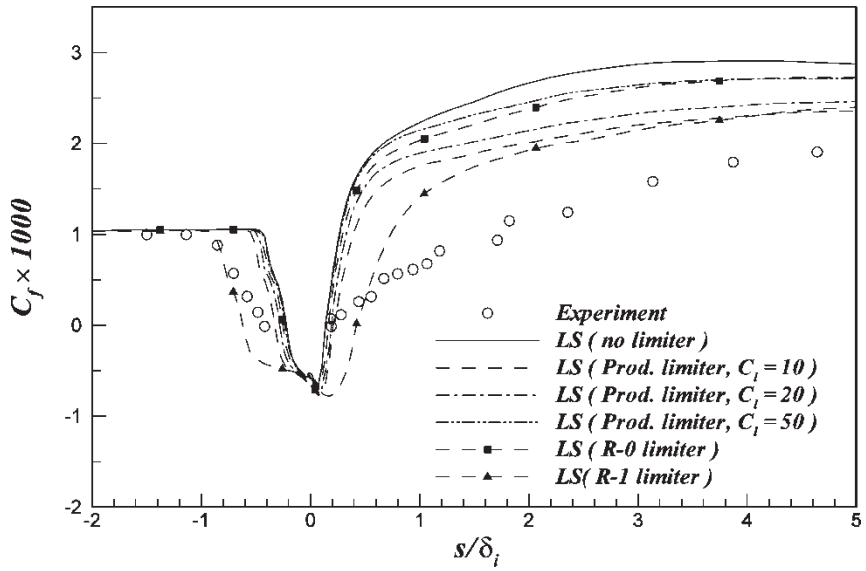

Figure 5. Distributions of skin friction coefficient.

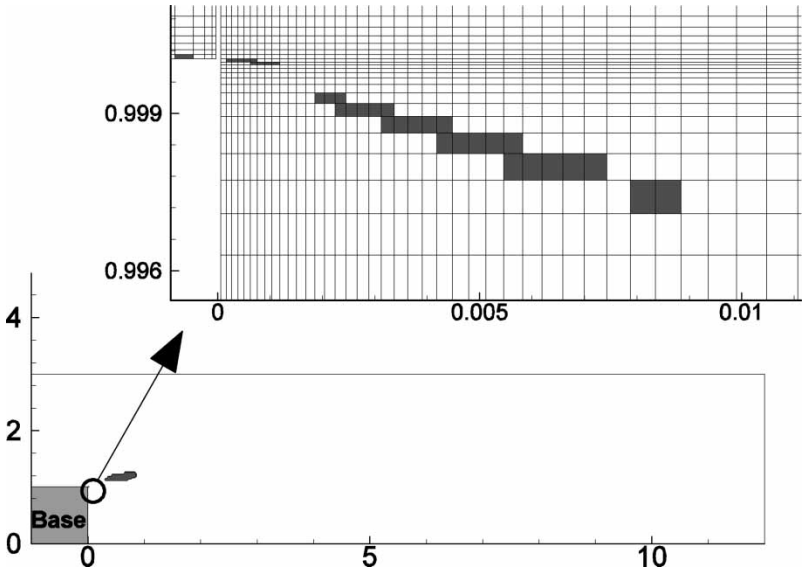

Figure 6. Supersonic base flow: Regions with non-realizable $\tilde{S}$.

Obviously, this is not the case for the compression ramp flow as can be seen from figure 5.

4.3 Supersonic base flow

A compressible axisymmetric Navier–Stokes code with the LS turbulence model was used in the present calculation of supersonic base flow. The target flow was Herrin and Dutton (1991)'s base flow having a freestream Mach number of 2.46. Computational domain, non-dimensionalized by the base radius, extended from -1 to 12 for x/R and from 0 to 3 for r/R. The computational domain was divided into two blocks as sketched in figure 6. We chose a 21 × 50 and 200 × 150 grid system for each block through the grid-test. A more detailed description of the numerical method including the boundary conditions are given in Kim and Park (1998).

It was not possible to obtain a converged solution if no limiter was employed. Converged solutions, obtained by the R-0 limiter and the Menter's limiter with $C_l = 10{,}20$ and 50, were found to be almost equal to one another. We conjecture that this is due to the fact that the region where unphysical turbulence values appear is very small compared to the overall flow domain. Figure 6 shows the regions where the non-dimensional strain rate $\tilde{S}$ does not comply with the condition of equation (26) with $C_\mu = 0.09$, as extracted from the solution filed using the R-0 limiter. We see that these regions are very small and belong to the mixing layer region (figure 6 top) and the expansion wave region (figure 6 bottom) near the corner.

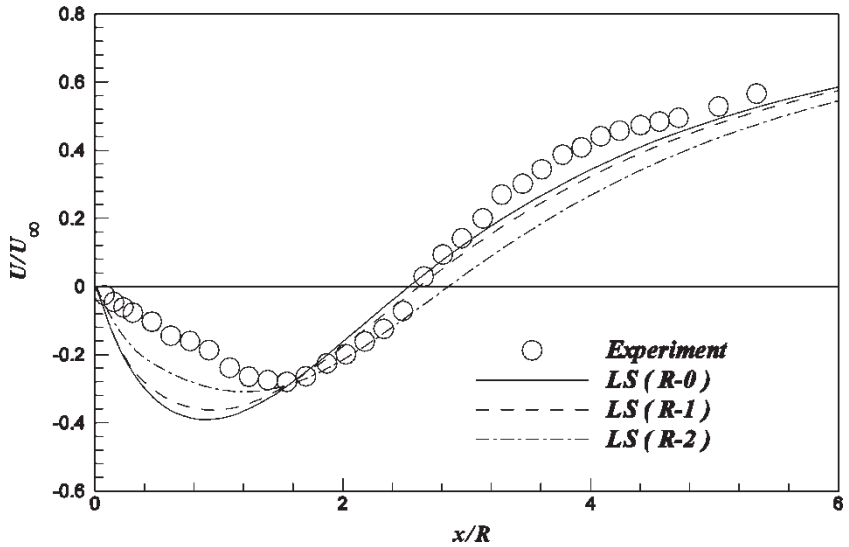

Figure 7. Mean axial velocity distributions along the centerline.

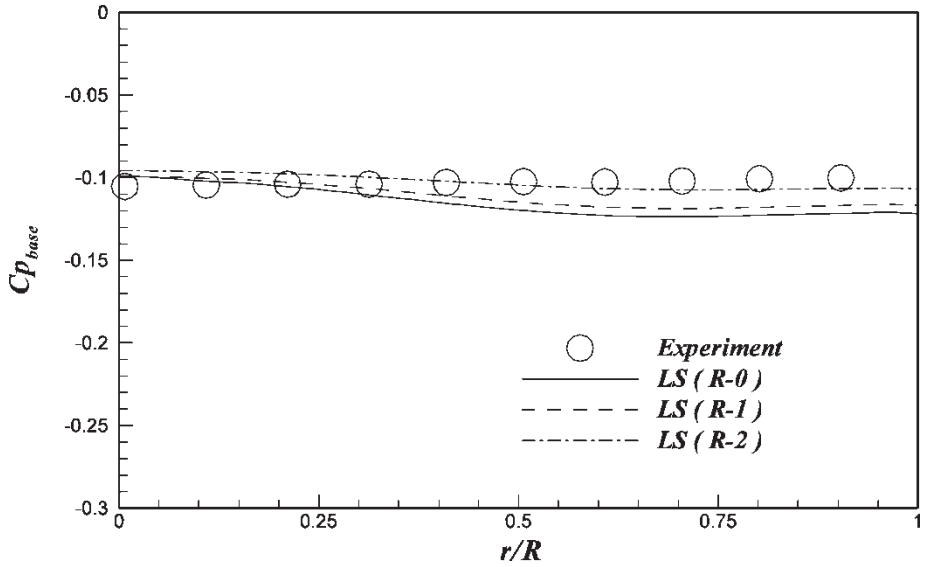

Figure 8. Base pressure distributions.

Figures 7 and 8 illustrate how the mean axial velocity along the centerline and the base pressure vary with the choice of various limiters. As seen in the case of compression ramp flow, the predictions vary substantially by the choice of limiters. A general trend of the predicted axial velocity profile is that the model that performs better in the recirculation zone performs poorer in the downstream region of reattachment. It is interesting to see that the closeness of the predictions to the experimental data in base pressure (figure 8) goes with the performance of each limiter in predicting the axial velocity in the recirculation region.

5. Conclusions

From the realizability condition, a mathematically correct bound for eddy viscosity in linear two-equation turbulence models was obtained by using the geometrical relations. From this, the realizability bounds for turbulent time scale, production rate of TKE, non-equilibrium factor and non-dimensional strain rate were also obtained. These bounds can be used advantageously to obtain a converged solution. The effects of various limiters on some simple flows have been studied. It has been demonstrated that the solutions vary substantially by the choice of limiters, which is quite disturbing for practitioners. It is therefore recommended that the limiters used in the simulation should be explicitly pointed out to make the computational results reliable and repeatable.

References

Behnia, M., Parneix, S. and Durbin, P.A. Simulation of jet impingement heat transfer with the $k - \varepsilon - \nu^2$ model. Annual Research Briefs 1996, pp. 3–16, 1996 (CTR: Stanford, California), [http://ctr.stanford.edu/resbriefs96/behnia.ps.z">www http://ctr.stanford.edu/ResBriefs96/behnia.ps.z].

Behnia, M., Parneix, S. and Durbin, P.A. Prediction of heat transfer in an axisymmetric turbulent jet impinging on a flat plate. *Int. J. Heat Mass Trans.*, 1998, **41**(12), 1845–1855.

Durbin, P.A. On the stagnation point anomaly. *Int. J. Heat Fluid Fl.*, 1996, **17**(1), 89–90.

Durbin, P.A. and Pettersson Reif, B.A. Statistical theory and modeling for turbulent flows, pp. 136–138, 2001 (John-Wiley & Sons: New York, NY).

Herrin, J.L. and Dutton, J.C. An experimental investigation of the supersonic axisymmetric base flow behind a clindrical afterbody, 1991 (University of Illinois: Urbana-Champaiga, UILU 91-4004, Urbana, IL).

Ilinca, F. and Pelletier, D. Positivity preservation and adaptive solution for the $k - \varepsilon$ model of turbulence. *AIAA J.*, 1998, **36**(1), 44–50.

Jacon, F., Knight, D. 1994 "A Navier–Stokes algorithm for turbulent flows using an unstructured grid and flux differencing splitting", AIAA Paper 94-2293.

Kim, M.H. and Park, S.O. Supersonic base flow predictions using second-moment closure models of turbulence. *CFD J.*, 1998, **6**(4), 561–576.

Kral, L.D., Mani, M. and Ladd, J.A. Application of turbulence models for aerodynamic and propulsion flowfields. *AIAA J.*, 1996, **34**(11), 2291–2298.

Launder, B.E. and Sharma, B.I. Application of the energy dissipation model of turbulence to the calculation of flow near a spinning disc. *Lett. Heat Mass Trans.*, 1974, **1**(2), 131–138.

Lee, C.H. and Park, S.O. Computations of hypersonic flows over blunt body using a modified low-diffusion flux-splitting scheme. *CFD J.*, 2002, **10**(4), 490–500.

Liu, F. and Zheng, X. A strongly coupled time-marching method for solving the Navier–Stokes and $k - \omega$ turbulence model equations with multigrid. *J. Comput. Phys.*, 1996, **128**, 289–300.

Luo, H., Baum, J., Lohner, R. (1997) "Computation of compressible flows using a two-equation turbulence model on unstructured grids", AIAA Paper 97-0430.

Medic, G. and Durbin, P.A. Toward improved prediction of heat transfer on turbine blades. *ASME J. Turbomach.*, 2002, **124**, 187–192.

Menter F.R. 1993 "Zonal two-equation $k - \omega$ models for aerodynamics flow", AIAA Paper 93-2906.

Moore, J.G., Moore, J. (1999) "Realizability in two-equation turbulence models", AIAA Paper 99-3779.

Shur M., Strelets, M., Zaikov, L., Gulyaev, A., Kozlov, V., Secundov, A. 1995 "Comparative testing of one- and two-equation turbulence models for flows with separation and reattachment", AIAA Paper 95-0863.

Smits, A.J. and Muck, K.C. "Experimental study of three shock wave/turbulent boundary layer interactions", *J. Fluid Mech.*, 1987, **182**, 291–314.

Thivet, F. 2002 “Lessons learned from RANS simulations of shock-wave/boundary-layer interactions”, AIAA Paper 2002-0583.
Thivet, F., Knight, D.D. Zheltovodov, A.A. and Maksimov, A.I., Insights in turbulence modeling for crossing-shock-wave/boundary-layer interactions. *AIAA J.*, 2001, **39**(6), 985–995.
Wilcox, D.C. *Turbulence Modeling for CFD*, 2nd Ed., 1998, (DCW Industries, Inc., (La Canada, CA).
Yoon, B.K., Chung, M.K. and Park, S.O. Comparisons between low Reynolds number two-equation models for computation of a shockwave-turbulent-boundary layer interaction. *The Aeronaut. J.*, 1997, **101**(1007), 335–345.
Zheng, X. and Liu, F. Staggered upwind method for solving Navier–Stokes and $k - \omega$ turbulence model equations. *AIAA J.*, 1995, **33**(6), 991–998.